

3-27-2017

# Lifetimes in $^{124}$Te: Examining Critical-Point Symmetry in the Te Nuclei

S. F. Hicks
*University of Dallas*

J. R. Vanhoy
*United States Naval Academy*

P. G. Burkett
*University of Dallas*

B. R. Champine
*United States Naval Academy*

S. J. Etzkorn
*University of Dallas*

***See next page for additional authors***

# Lifetimes in $^{124}$Te: Examining critical-point symmetry in the Te nuclei

S. F. Hicks,[1,*] J. R. Vanhoy,[2] P. G. Burkett,[1] B. R. Champine,[2] S. J. Etzkorn,[1]
P. E. Garrett,[3,4] S. W. Yates,[3,5] and Minfang Yeh[5,6]

[1]*Department of Physics, University of Dallas, Irving, Texas 75062-4736, USA*
[2]*Department of Physics, United States Naval Academy, Annapolis, Maryland 21402-5026, USA*
[3]*Department of Physics and Astronomy, University of Kentucky, Lexington, Kentucky 40506-0055, USA*
[4]*Department of Physics, University of Guelph, Guelph, Ontario, NOB 1S0, Canada*
[5]*Department of Chemistry, University of Kentucky, Lexington, Kentucky 40506-0055, USA*
[6]*Department of Chemistry, Brookhaven National Laboratory, Upton, New York, 11973-5000, USA*

(Received 5 September 2016; revised manuscript received 5 February 2017; published 27 March 2017)

The Doppler-shift attenuation method following inelastic neutron scattering was used to determine the lifetimes of nuclear levels to 3.3-MeV excitation in $^{124}$Te. Level energies and spins, $\gamma$-ray energies and branching ratios, and multipole-mixing ratios were deduced from measured $\gamma$-ray angular distributions at incident neutron energies of 2.40 and 3.30 MeV, $\gamma$-ray excitation functions, and $\gamma\gamma$ coincidence measurements. The newly obtained reduced transition probabilities and level energies for $^{124}$Te were compared to critical-point symmetry model predictions. The $E(5)$ and $\beta^4$ potential critical-point symmetries were also investigated in $^{122}$Te and $^{126}$Te.

DOI: 10.1103/PhysRevC.95.034322

## I. INTRODUCTION

The underlying structure of $^{124}$Te has proven to be difficult to characterize, notwithstanding a variety of experimental and theoretical investigations [1–13]. Structural ambiguities for the Te isotopic chain are readily apparent when one examines the mass dependence of selected levels. The $2_1^+$-, $4_1^+$-, and $2_2^+$-level energies show the expected spacing and increase for vibrational states as the neutron number increases above mid-shell $N = 66$. The $6_1^+$ level, however, remains at a nearly constant excitation energy, indicative of a state dominated by two-proton configurations relatively unaffected by the addition of neutrons [3,4,14]. The ratio $E(4_1^+)/E(2_1^+) = 2.07$ in $^{124}$Te is very near the harmonic value of 2, but the energy spread of the two-phonon multiplet and the high energy of the $0_2^+$ state do not support a simple vibrational picture.

The quadrupole moments of the $2_1^+$ levels in the even-mass stable Te nuclei are nonzero and comparable in magnitude to those observed in rotational nuclei [13]. For $^{124}$Te, other characteristics such as the $0_2^+$ level energy hint at $O(6)$, or $\gamma$-soft rotational behavior as well, but the $E(4_1^+)/E(2_1^+)$ ratio is expected to be 2.5 for such structure; furthermore, the decay characteristics of the $0_2^+$ level are not those predicted for an $O(6)$ nucleus. The evaluation of recent $^{120,122,124}$Te Coulomb excitation results with interacting boson model (IBM) and large-scale shell model (LSSM) calculations has provided further supporting evidence of the soft-triaxial nature of $^{124}$Te [12]. However, an even more recent study of energy spectra and transition probabilities in $^{118-128}$Te using the IBM indicates that while $\gamma$-soft rotor features exist in the Te isotopes, their structure is mainly vibrational, with both $^{124}$Te and $^{126}$Te exhibiting $E(5)$ critical-point symmetry [13].

Critical-point symmetries were introduced by Iachello [15,16] to help describe transitional nuclei. He used Bohr's geometric model [17] to explain the phase transition at the critical point between vibrational and $\gamma$-soft nuclei ($U(5) \rightarrow O(6)$ within the IBM) and denoted this symmetry as $E(5)$. At the critical point, the potential energy $U(\beta,\gamma)$ of the geometric Hamiltonian becomes independent of $\gamma$, and the wave function is separable in the $\beta$ and $\gamma$ degrees of freedom. Relative energies and transition rates are determined in closed form, and the excited-state energies and transition rates for a given nucleus scale using the experimental values of $E(2_1^+)$ and $B(E2; 2_1^+ \rightarrow 0_1^+)$ [15,18]. The first empirical evidence of the $E(5)$ dynamical symmetry was reported in $^{134}$Ba by Casten and Zamfir [19].

Arias *et al.* [20] investigated the relationship between IBM predictions for this same phase transition and the $E(5)$ symmetry. They determined that a potential energy $U(\beta) \propto \beta^4$ gives predictions for the phase transition which were identical to the IBM predictions in the many-boson limit, and closer to the IBM predictions in the few-boson limit than those of the $E(5)$ dynamic symmetry; closed-form solutions for energies and transition rates for $U(\beta) \propto \beta^4$ are found in Ref. [20].

In a search for $E(5)$ behavior $^{124}$Te was proposed as one of the six best candidates, along with $^{102}$Pd, $^{106,108}$Cd, $^{128}$Xe, and $^{134}$Ba [18]. With its re-emergence as a good $E(5)$ candidate nucleus [13], a more comprehensive investigation of its structure was warranted.

The level scheme of $^{124}$Te has been fairly well established to over 3 MeV in previous experimental investigations [3,5,6,8–11]. Level energies and spins, which have been the focus of much of the previous experimental work, are not sufficient to answer many questions regarding underlying dynamical symmetries and other structural properties; rather wave-function sensitive information, such as electromagnetic transition probabilities, is needed. Lifetimes are known for some states in $^{124}$Te [5,8,11], but a deficiency in this essential information remains for many low-lying levels. Identifying the critical-point symmetries depends on key observables that are discussed in detail in Ref. [18], but must include the

*hicks@udallas.edu

 

identification of $0^+$ levels and the determination of $B(E2)$ values for transitions between low-lying, positive-parity levels.

In this investigation of the structure of $^{124}$Te, the nonselective $(n,n'\gamma)$ reaction was utilized to examine levels to 3.3-MeV excitation. In particular, the Doppler-shift attenuation method following inelastic neutron scattering was used to determine lifetimes in the range of a few fs to approximately 1 ps for many low-energy $^{124}$Te levels with $J < 6$. These measurements provide many new reduced transition probabilities for examining whether $^{124}$Te is a nucleus exhibiting critical-point symmetry. For completeness, critical-point phenomena are also investigated in neighboring $^{122}$Te and $^{126}$Te, for which lifetimes were obtained using the same experimental techniques and reported previously [21,22].

## II. EXPERIMENTAL METHOD AND DATA REDUCTION

Measurements were made using the neutron scattering facilities at the University of Kentucky Accelerator Laboratory (UKAL), where the $^3$H$(p,n)^3$He reaction was used as a neutron source. The 19.3-g powdered $^{124}$Te sample, isotopically enriched to 94%, was packed into a thin-walled polyethylene container with diameter of 1.85 cm and height of 2.90 cm.

For $\gamma\gamma$ coincidence measurements, neutrons emerging from the source reaction were formed into a 1-cm beam by the use of a lithium-loaded collimator approximately 75 cm long. The sample was hung coaxially with this beam, and four HpGe detectors with ∼50% relative efficiency were placed in a coplanar arrangement approximately 6 cm from the center of the sample. Data were stored in event mode, and a two-dimensional matrix was constructed off-line by considering pairwise coincidences. A portion of the coincidence spectrum gated by the 646-keV $\gamma$ ray from the $4_1^+$ state is shown in Fig. 1. The coincidence setup was described in detail in Ref. [23].

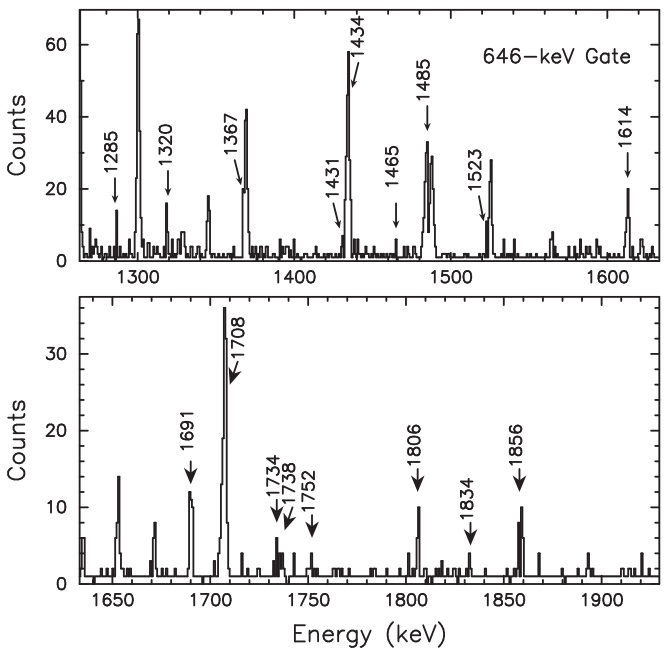


FIG. 1. Portions of the $\gamma\gamma$ coincidence spectrum from a gate set on the 646-keV $\gamma$ ray from the $4_1^+ \rightarrow 2_1^+$ transition in $^{124}$Te.

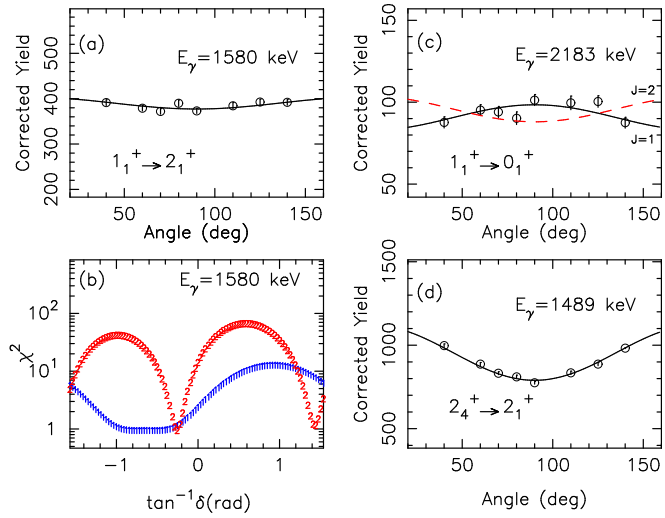


FIG. 2. Angular distributions of emitted $\gamma$ rays from excited levels in $^{124}$Te are shown in Figs. 2(a), 2(c), and 2(d). The $\chi^2$ vs $\tan^{-1}(\delta)$ curve shown in Fig. 2(b) is for the 1580-keV $\gamma$ ray from the 2183-keV level. The 2183-keV level has previously been reported as having a spin of both $J = 1$ [9] and $J = 2$ [11]. The $J = 1$ and $J = 2$ possible spin solutions are shown by the solid and dashed lines, respectively, in Fig. 2(c).

$\gamma$-ray excitation functions, angular distributions, and Doppler shifts were measured with a single $\gamma$-ray detector. For this arrangement, a Compton-suppressed $n$-type HpGe detector with 51% relative efficiency and an energy resolution of about 2.1 keV FWHM at 1.33 MeV was used. A bismuth germanate (BGO) annular detector surrounding the main detector was used for Compton suppression and as an active shield. The gain stability of the system was monitored using radioactive $^{56}$Co and $^{152}$Eu sources, which were also used to determine the detector efficiency and energy calibrations. The neutron scattering facilities, time-of-flight neutron background suppression, neutron monitoring, and data reduction techniques have been described elsewhere [24].

$\gamma$-ray yields were measured at incident neutron energies of 2.4 and 3.3 MeV and angles between 40° and 140°. These angular distributions were fit to even-order Legendre polynomial expansions and compared to calculations from the statistical model code CINDY [25] in order to extract multipole-mixing ratios and level spins.

The angular distribution of the 1580-keV $\gamma$ ray from the 2183-keV level is shown in Fig. 2(a). From the $\chi^2$ versus $\tan^{-1}\delta$ curve for this same $\gamma$ ray shown in Fig. 2(b), $J_i = 1$ and $J_i = 2$ are possible spins for the 2183-keV level; the multipole-mixing ratio for the 1580-keV $\gamma$ ray is obtained from the $\chi^2$ minimum in Fig. 2(b). The angular distribution of the $\gamma$ ray resulting from the decay to the ground state of this same level is shown in Fig. 2(c); its shape shows clearly the spin of the level is $J_i = 1$ (solid line), as opposed to $J = 2$ (dashed line). The angular distribution of the 1489-keV $\gamma$ ray is shown in Fig. 2(d).

$\gamma$-ray excitation functions, measured at incident neutron energies between 2.2 and 3.3 MeV in ≈ 75 keV steps, were used to place $\gamma$ rays in the level decay scheme, to assist in

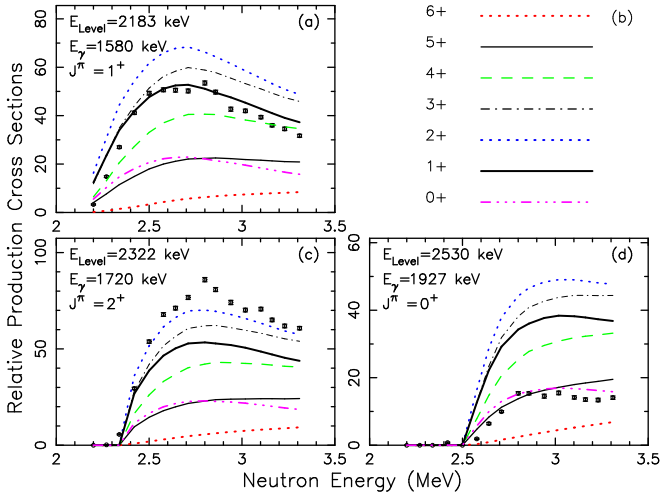


FIG. 3. Relative $\gamma$-ray production cross sections observed in $^{124}$Te compared to statistical model calculations are shown. Data and calculations shown in Figs. 3(a), 3(c), and 3(d) were used to clarify the spin of the 2083-keV level, verify a $2^+$ level at 2322 keV, and identify a new $0^+$ level at 2530, respectively. The legend for the model calculations for different spins is shown in Fig. 3(b).

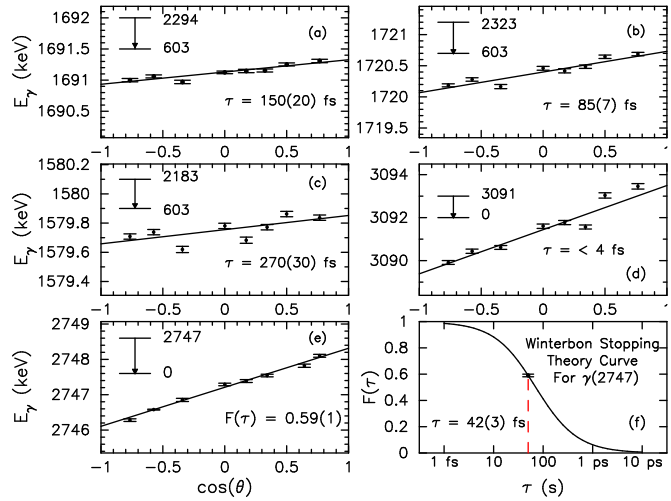


FIG. 4. Doppler shifts for several $\gamma$ rays in $^{124}$Te are shown in Figs. 4(a)–4(d). The Doppler shifts and the experimental $F(\tau)$ value for the 2747-keV $\gamma$ ray are shown in Fig. 4(e), while the theoretical $F(\tau)$ curve generated using the Winterbon formalism is shown in Fig. 4(f), with the dashed line showing the extrapolated lifetime.

making spin assignments, and to determine branching ratios. Theoretical cross sections were calculated using the statistical model code CINDY [25] with optical model parameters appropriate for this mass and energy region [26]. Experimental $\gamma$-ray production cross sections were then compared to theoretical values for each level to assess level spins and $\gamma$-ray branching ratios. Sample experimental and calculated excitation functions are shown in Fig. 3. The good agreement between calculations and data support the branching ratios and spin assignments of the levels. The larger 2322-keV $2^+$-level production cross sections observed relative to the statistical model calculations are common for states with significant feeding.

Level lifetimes were extracted using the Doppler-shift attenuation method following inelastic neutron scattering as discussed in Ref. [28]. By comparing experimental and theoretical Doppler-shift attenuation factors, the experimental $F(\tau)$ value was determined using

$$E_\gamma(\theta) = E_0\left[1 + F(\tau)\frac{v_{\text{c.m.}}}{c}\cos\theta\right], \quad (1)$$

where $E_\gamma(\theta)$ is the $\gamma$-ray energy as a function of detection angle relative to the incident beam direction, $E_0$ is the unshifted $\gamma$-ray energy, $v_{\text{c.m.}}$ is the center-of-mass velocity of the recoiling nucleus, and $c$ is the speed of light.

Theoretical attenuation factors $F(\tau)$ were calculated using the stopping theory of Winterbon [27], as described in Ref. [28]. The experimental Doppler shifts and the theoretical shifts used to extract the lifetime for the 2747-keV level are shown in the bottom two panels of Fig. 4; other selected Doppler shifts are also shown. Comparisons of lifetimes obtained in this work with those from previous measurements [8,11] are given in Table I. The adopted lifetimes of the $2_1^+$ and $4_1^+$ levels are included for completeness. A range of lifetimes for the $4_1^+$ level of 1000 fs $< \tau <$ 6700 fs, along with a best-fit value was found in Ref. [8]; it is the latter value that is adopted in Ref. [11].

## III. RESULTS

Level spin and parity assignments, level energies, $\gamma$-ray placements, $\gamma$-ray branchings, multipole-mixing ratios, level lifetimes, and transition rates for all observed levels to 3.3-MeV excitation are given in Table II. Information on low-lying $2^+$ levels was reported previously in Ref. [29] but is included here for completeness. Only those levels that merit special attention are discussed below.

New levels are indicated by an $l$ and new transitions by an $i$ in the notes column of Table II. Some of the levels above

TABLE I. Comparisons of $^{124}$Te level lifetimes measured in this work with those from Refs. [8] and [11]. The adopted values for the 1657-, 2039-, and 2092-keV levels are those of Ref. [8].

| Level (keV) | Adopted [11] (ps) | GRID [8] (ps) | $(n,n'\gamma)$ (ps) |
|---|---|---|---|
| 602.73 | $8.9^{+1}_{-1}$ | | |
| 1248.59 | | $2.0^{+20}_{-7}$ | |
| 1325.52 | | $1.5^{+3}_{-2}$ | $0.85^{+17}_{-13}$ |
| 1656.67 | | $0.8^{+2}_{-1}$ | $1.2^{+3}_{-2}$ |
| 2039.29($2^+$) | | $0.7^{+2}_{-1}$ | $0.88^{+11}_{-11}$ |
| 2092.03 | | $0.4^{+1}_{-1}$ | $0.74^{+12}_{-10}$ |
| 2293.73 | $0.25^{+9}_{-9}$ | | $0.15^{+2}_{-2}$ |
| 2747.05 | $0.039^{+4}_{-4}$ | | $0.042^{+3}_{-3}$ |
| 2782.4 | $0.33^{+10}_{-10}$ | | $0.083^{+7}_{-6}$ |
| 2974.91 | $0.094^{+13}_{-13}$ | | $0.051^{+5}_{-5}$ |

TABLE II. Levels and transition rates in $^{124}$Te. Uncertainties are in the last digit(s). The adopted energy of the $2_1^+$ state was used for level development [11]. An $E1$ in the mixing ratio column indicates that a $B(E1)$ value is given in the $B(M1)/B(E1)$ column. The mixing ratios and $B(XL)s$ presented are those of the first spin listed when the spin of the initial state is not definite, and when two mixing ratios are listed, the one with the lowest $\chi^2$ is listed first. Square brackets [ ] indicate a tentative assignment.

| $J^\pi$ | $E_x$ (keV) | $E_\gamma$ (keV) | Note | $E_f$ (keV) | BR (%) | $\delta$[a] | $\tau$ (fs) | $B(M1)/B(E1)$ (W.u.[b])/(W.u.)[c] | $B(E2)$ (W.u.)[d] |
|---|---|---|---|---|---|---|---|---|---|
| $2^+$ | 602.73(1) | 602.73(1) | | 0 | 100 | | $8900^{+140e}_{-140}$ | | $31.1^{+5e}_{-5}$ |
| $4^+$ | 1248.59(5) | 645.86(5) | | 603 | 100 | | | | $35.9^{+17f}_{-17}$ |
| $2^+$ | 1325.52(6) | 722.79(4) | | 603 | 87(1) | $-0.49^{+5}_{-3}$ | $850^{+170}_{-130}$ | $6.9^{+15}_{-13}\times10^{-2}$ | $22.1^{+45}_{-43}$ |
| | | | | | | $-0.96^{+1}_{-1}$ | | $4.5^{+9}_{-8}\times10^{-2}$ | $55.5^{+109}_{-99}$ |
| | | 1325.51(5) | | 0 | 13(1) | | | | $8.3^{+23}_{-16}\times10^{-1}$ |
| $0^+$ | 1656.67(11) | 1053.94(11) | | 603 | 100 | | $1200^{+300}_{-200}$ | | $14.3^{+29}_{-29}$ |
| $6^+$ | 1747.40(7) | 499.53(5) | | 1249 | 100 | | | | |
| $0^+$ | 1883.07(7) | 557.59(4) | | 1326 | 100 | | | | |
| $4^+$ | 1957.92(8) | 632.39(10) | g | 1326 | 3(1) | | $520^{+110}_{-80}$ | | $12.7^{+74}_{-58}$ |
| | | 709.32(5) | | 1249 | 51(1) | $-0.36^{+3}_{-3}$ | | $7.7^{+17}_{-15}\times10^{-2}$ | $14.1^{+30}_{-28}$ |
| | | 1355.18(7) | | 603 | 46(1) | | | | $4.3^{+9}_{-9}$ |
| $3^+$ | 2039.28(9) | 713.78(5) | h,j | 1326 | 49(1) | | | | |
| | | 790.71(2) | j | 1249 | 17(1) | | | | |
| | | 1436.56(9) | j | 603 | 34(1) | | | | |
| $2^+$ | 2039.29(8) | 382.29(5) | | 1657 | $< 1$ | | $880^{+110}_{-110}$ | | $< 69$ |
| | | 713.78(5) | h,j | 1326 | 2(1) | | | | |
| | | 790.71(2) | j | 1249 | 1(1) | | | | $8.1^{+104}_{-81}\times10^{-1}$ |
| | | 1436.56(9) | j | 603 | 61(1) | | | | |
| | | 2039.30(7) | | 0 | 36(1) | | | | $2.6^{+5}_{-4}\times10^{-1}$ |
| $2^+$ | 2092.03(9) | 766.33(10) | h | 1326 | 1(1) | $+0.58^{+42}_{-92}$ | $740^{+120}_{-100}$ | $1.2^{+18}_{-13}\times10^{-3}$ | $2.9^{+39}_{-33}\times10^{-1}$ |
| | | 1489.03(9) | | 603 | 92(1) | $+0.85^{+2}_{-2}$ | | $6.9^{+12}_{-11}\times10^{-3}$ | $1.6^{+3}_{-3}$ |
| | | | | | | $+0.06^{+3}_{-3}$ | | $1.2^{+3}_{-3}\times10^{-2}$ | $1.4^{+3}_{-3}\times10^{-2}$ |
| | | 2091.75(7) | | 0 | 7(1) | | | | $5.3^{+17}_{-14}\times10^{-2}$ |
| $0^+$ | 2153.37(8) | 827.83(6) | | 1326 | 81(1) | | $> 1$ ps | | $< 50$ |
| | | 1550.30(10) | | 603 | 19(1) | | | | $< 5\times10^{-1}$ |
| $1^+$ | 2182.54(8) | 856.90(8) | | 1326 | 9(1) | $+0.22^{+106}_{-146}$ | $270^{+30}_{-30}$ | $1.6^{+10}_{-7}\times10^{-2}$ | $7.4^{+38}_{-38}\times10^{-1}$ |
| | | 1579.78(7) | | 603 | 73(1) | $-0.49^{+25}_{-32}$ | | $1.8^{+5}_{-5}\times10^{-2}$ | $1.2^{+4}_{-3}$ |
| | | 2182.61(10) | | 0 | 18(1) | | | $2.0^{+3}_{-3}\times10^{-3}$ | |
| $4^+$ | 2224.96(6) | 899.80(7) | | 1326 | 12(1) | | $340^{+100}_{-70}$ | | $13.4^{+49}_{-39}$ |
| | | 976.23(6) | | 1249 | 56(1) | $+0.44^{+11}_{-14}$ | | $4.7^{+17}_{-13}\times10^{-2}$ | $6.7^{+23}_{-20}$ |
| | | 1622.40(6) | | 603 | 32(1) | | | | $1.9^{+6}_{-5}$ |
| $3^-$ | 2293.73(7) | 335.44(10) | | 1958 | $< 1$ | $E1$ | $150^{+20}_{-20}$ | $< 7\times10^{-4}$ | |
| | | 968.20(8) | | 1326 | 3(1) | $E1$ | | $9^{+5}_{-4}\times10^{-5}$ | |
| | | 1045.09(8) | | 1249 | 5(1) | $E1$ | | $1.1^{+4}_{-3}\times10^{-4}$ | |
| | | 1690.98(6) | | 603 | 92(1) | $E1$ | | $4.9^{+8}_{-6}\times10^{-4}$ | |
| $0^+$ | 2308.10(8) | 1705.28(7) | | 603 | 100 | | $170^{+40}_{-30}$ | | $9.1^{+20}_{-18}$ |
| $2^+$ | 2323.25(8) | 997.00(6) | g | 1326 | 2(1) | $-0.36^{+18}_{-22}$ | $85^{+7}_{-7}$ | $6.7^{+43}_{-37}\times10^{-3}$ | $6.1^{+40}_{-34}\times10^{-1}$ |

TABLE II. *(Continued.)*

| $J^\pi$ | $E_x$ (keV) | $E_\gamma$ (keV) | Note | $E_f$ (keV) | BR (%) | $\delta$[a] | $\tau$ (fs) | $B(M1)/B(E1)$ (W.u.[b])/(W.u.)[c] | $B(E2)$ (W.u.)[d] |
|---|---|---|---|---|---|---|---|---|---|
| | | 1720.30(7) | | 603 | 96(2) | $-0.03^{+9}_{-3}$ | | $7.0^{+8}_{-7} \times 10^{-2}$ | $6.0^{+7}_{-6} \times 10^{-2}$ |
| | | | | | | $0.86^{+4}_{-3}$ | | $4.1^{+5}_{-5} \times 10^{-2}$ | $7.1^{+9}_{-8}$ |
| | | 2323.10(32) | | 0 | 2(1) | | | | $7.8^{+50}_{-42} \times 10^{-2}$ |
| $5^-$ | 2334.6(17) | 377.88(7) | | 1958 | 3(1) | $E1$ | $> 1$ ps | $< 3 \times 10^{-4}$ | |
| | | 1086.70(16) | | 1249 | 97(1) | $E1$ | | $< 3 \times 10^{-4}$ | |
| $6^+$ | 2348.7(13) | [602.38(10)] | | 1747 | | | | | |
| | | 1101.04(12) | | 1249 | | | | | |
| $2^+$ | 2453.83(5) | 1128.27(3) | g | 1326 | 12(1) | $-0.79^{+28}_{-16}$ | $360^{+40}_{-40}$ | $4.5^{+16}_{-11} \times 10^{-3}$ | $1.6^{+5}_{-5}$ |
| | | 1205.54(12) | | 1249 | 7(1) | | | | $1.7^{+5}_{-4}$ |
| | | 1851.50(5) | | 603 | 64(1) | $+0.16^{+18}_{-13}$ | | $8.7^{+14}_{-12} \times 10^{-3}$ | $4.6^{+8}_{-6} \times 10^{-2}$ |
| | | | | | | $+0.79^{+06}_{-09}$ | | $5.5^{+11}_{-11} \times 10^{-3}$ | $7.0^{+13}_{-12} \times 10^{-1}$ |
| | | 2454.40(10) | | 0 | 17(1) | | | | $1.2^{+3}_{-2} \times 10^{-1}$ |
| $(4)^{(-)}$ | 2483.3(9) | 443.96(6) | h | 2039(3) | | | | | |
| | | 525.41(7) | | 1958 | | | | | |
| | | 1234.7(7) | j | 1249 | | | | | |
| $4^+$ | 2511.89(6) | 1263.16(6) | | 1249 | 94(1) | $+0.75^{+5}_{-2}$ | $1040^{+440}_{-250}$ | $9.1^{+31}_{-30} \times 10^{-3}$ | $2.6^{+9}_{-7}$ |
| | | 1909.59(11) | i | 603 | 6(1) | | | | $5.1^{+28}_{-22} \times 10^{-2}$ |
| $2^+$ | 2521.24(12) | 1195.86(10) | g | 1326 | 4(1) | $-0.22^{+146}_{-107}$ | $85^{+5}_{-5}$ | $8.3^{+51}_{-37} \times 10^{-3}$ | $2.0^{+10}_{-11} \times 10^{-1}$ |
| | | 1273.36(4) | i | 1249 | $<2(1)$ | | | | $< 1.6$ |
| | | 1918.40(12) | | 603 | 94(1) | $+0.86^{+4}_{-3}$ | | $2.9^{+3}_{-3} \times 10^{-2}$ | $4.0^{+4}_{-4}$ |
| | | | | | | $0.00^{+9}_{-6}$ | | $5.0^{+4}_{-4} \times 10^{-2}$ | $1^{+1}_{-1} \times 10^{-5}$ |
| $(0^+)$ | 2529.90(5) | 1927.10(5) | | 603 | 100 | | $480^{+140}_{-100}$ | | $1.7^{+5}_{-4}$ |
| (4) | 2549.10(8) | 1301.11(6) | k | 1249 | 100 | $+0.81^{+5}_{-7}$ | $170^{+20}_{-20}$ | $5.1^{+10}_{-7} \times 10^{-2}$ | $14^{+3}_{-3}$ |
| | 2568.93(11) | 1320.35(10) | i,l | 1249 | 100 | | | | |
| 5 | 2594.46(9) | 846.97(5) | | 1747 | 10(1) | | $> 1$ ps | | |
| | | 1345.73(5) | k | 1249 | 90(1) | $-0.64^{+14}_{-11}$ | | | |
| $1^+$ | 2601.40(12) | 943(1) | g | 1657 | 3(1) | | $160^{+20}_{-20}$ | $7.1^{+4}_{-3} \times 10^{-3}$ | |
| | | 1275.36(4) | | 1326 | 10(1) | $+0.72^{+36}_{-73}$ | | $6.3^{+45}_{-21} \times 10^{-3}$ | $1.4^{+7}_{-8}$ |
| | | 1997.92(7) | | 603 | 60(2) | $-0.13^{+138}_{-115}$ | | $1.5^{+7}_{-5} \times 10^{-2}$ | $4.4^{+17}_{-15} \times 10^{-2}$ |
| | | 2601.18(12) | | 0 | 27(2) | | | $3.0^{+7}_{-6} \times 10^{-3}$ | |
| (3) | 2618.2(10) | 1369.55(6) | g | 1249 | 74(2) | $-0.75^{+11}_{-23}$ | $770^{+1200}_{-300}$ | | |
| | | 2015.73(17) | | 603 | 26(2) | | | | |
| $1^+,2^+$ | 2640.84(40) | 1315.40(12) | | 1326 | | | | | |
| | | 2038.30(12) | j | 603 | | | | | |
| | | 2640(1) | m | 0 | | | | | |
| 6 | 2665.5(13) | 329.77(4) | g,h | 2335 | 50(5) | | | | |
| | | 918.10(5) | i | 1747 | 50(5) | $+0.86^{+17}_{-22}$ | | | |
| $2^+$ | 2681.53(8) | 2078.50(7) | | 603 | 92(1) | $+0.88^{+5}_{-3}$ | $42^{+3}_{-3}$ | $4.4^{+5}_{-5} \times 10^{-2}$ | $5.5^{+7}_{-5}$ |
| | | | | | | $-0.09^{+9}_{-8}$ | | $7.7^{+8}_{-7} \times 10^{-2}$ | $1.0^{+1}_{-1} \times 10^{-1}$ |

TABLE II. *(Continued.)*

| $J^\pi$ | $E_x$ (keV) | $E_\gamma$ (keV) | Note | $E_f$ (keV) | BR (%) | $\delta$[a] | $\tau$ (fs) | $B(M1)/B(E1)$ (W.u.[b])/(W.u.)[c] | $B(E2)$ (W.u.)[d] |
|---|---|---|---|---|---|---|---|---|---|
| | | 2682.00(11) | | 0 | 8(1) | | | | $3.1^{+7}_{-6} \times 10^{-1}$ |
| | 2682.90(20) | 1434.32(20) | j,i,l | 1249 | | | | | |
| $3^-$ | 2694.2(8) | 1368.16(6) | | 1326 | 24(3) | | | | |
| | | 1445.82(20) | | 1249 | 5(1) | | | | |
| | | 2091.21(7) | | 603 | 71(7) | | | | |
| $2^{(-)}$ | 2701.33(8) | 1375.85(6) | | 1326 | 94(1) | $E1$ | $360^{+50}_{-50}$ | $3.9^{+7}_{-5} \times 10^{-4}$ | |
| | | 2099.10(4) | | 603 | 6(1) | $E1$ | | $1^{+5}_{-5} \times 10^{-5}$ | |
| | 2709.5(15) | 2709.5(15) | h,i,l | 0 | | | | | |
| 3 | 2710.82(10) | 1385.20(11) | k | 1326 | 55(2) | $-0.09^{+9}_{-10}$ | $580^{+200}_{-130}$ | $1.1^{+4}_{-4} \times 10^{-2}$ | $3.3^{+12}_{-10} \times 10^{-2}$ |
| | | 1461.79(7) | | 1249 | 11(2) | | | | |
| | | 2108.08(6) | | 603 | 34(1) | $-0.13^{+13}_{-13}$ | | $2.0^{+7}_{-6} \times 10^{-3}$ | $5.2^{+18}_{-15} \times 10^{-3}$ |
| (5) | 2713.26(7) | 1464.93(4) | h,i,k | 1249 | 100 | $-0.99^{+2}_{-4}$ | $170^{+50}_{-40}$ | $3.0^{+10}_{-2} \times 10^{-5}$ | $9.6^{+34}_{-23}$ |
| (5,4) | 2733.99(15) | 1485.40(14) | i | 1249 | 100 | $+0.30^{+7}_{-6}$ | $53^{+9}_{-7}$ | $1.7^{+3}_{-3} \times 10^{-1}$ | $4.8^{+9}_{-8}$ |
| (4,5,6) | 2737.29(9) | 990.53(4) | | 1747 | | | | | |
| | | 1488.70(8) | j | 1249 | | | | | |
| $1^-$ | 2747.05(15) | 2144.32(16) | | 603 | 19(1) | $E1$ | $42^{+3}_{-3}$ | $1.8^{+2}_{-2} \times 10^{-4}$ | |
| | | 2746.90(15) | | 0 | 81(1) | $E1$ | | $3.7^{+3}_{-3} \times 10^{-4}$ | |
| (2,3,1) | 2767.7(4) | 2164.16(3) | i,k | 603 | 100 | $-0.46^{+17}_{-12}$ | $140^{+20}_{-20}$ | $1.1^{+3}_{-2} \times 10^{-2}$ | $1.7^{+34}_{-23} \times 10^{-1}$ |
| | | | | | | $-1.51^{+19}_{-16}$ | | $5.4^{+11}_{-9} \times 10^{-3}$ | $4.9^{+11}_{-8} \times 10^{-1}$ |
| $6^+$ | 2774.28(8) | 1026.88(6) | h | 1747 | 50(5) | $-0.94^{+25}_{-11}$ | $< 4$ fs | | |
| | | 1526.18(5) | j | 1249 | 50(5) | | | | |
| $(3)^-$ | 2774.98(6) | 480.61(20) | h,k | 2294 | 5(1) | | | | |
| | | 735.32(6) | | 2039(3) | 16(1) | | | | |
| | | [816.80(9)] | | 1958 | 13(1) | | | | |
| | | 1526.18(6) | j | 1249 | 66(1) | | | | |
| $1^+$ | 2782.4(7) | 2179.08(20) | i,k | 603 | 12(3) | $-0.70^{+186}_{-62}$ | $83^{+7}_{-6}$ | $3.0^{+43}_{-16} \times 10^{-3}$ | $2.2^{+13}_{-27} \times 10^{-1}$ |
| | | 2782.89(8) | | 0 | 88(3) | | | $1.6^{+2}_{-2} \times 10^{-2}$ | |
| (3) | 2787.29(8) | 1461.79(7) | i,k,l | 1326 | 71(5) | | | | |
| | | 2184.0(8) | j,i | 603 | 29(5) | | | | |
| $2^+$ | 2808.89(12) | 627.29(5) | i | 2183 | 8(2) | $-0.54^{+36}_{-26}$ | $510^{+110}_{-70}$ | $1.5^{+8}_{-7} \times 10^{-2}$ | $8.1^{+44}_{-38}$ |
| | | 2205.40(13) | | 603 | 35(2) | $+0.54^{+15}_{-18}$ | | $1.6^{+5}_{-5} \times 10^{-3}$ | $6.6^{+19}_{-19} \times 10^{-2}$ |
| | | 2809.10(12) | | 0 | 58(2) | | | | $1.4^{+3}_{-3} \times 10^{-1}$ |
| $4^+$ | 2814.7(9) | 775.26(4) | k | 2039(3) | 35(4) | $+0.39^{+13}_{-9}$ | $> 2$ ps | $< 1.2 \times 10^{-2}$ | $< 2.1$ |
| | | 1565.92(5) | | 1249 | 57(4) | $+0.81^{+5}_{-5}$ | | $< 1.5 \times 10^{-3}$ | $< 2.9 \times 10^{-1}$ |
| | | 2211.8(20) | i | 603 | 8(2) | | | | $< 2.2 \times 10^{-2}$ |
| $(2,3,4^+)$ | 2816.95(7) | 2214.29(6) | k | 603 | 100 | $+0.87^{+7}_{-8}$ | $110^{+20}_{-20}$ | $1.5^{+5}_{-3} \times 10^{-2}$ | $1.6^{+5}_{-4}$ |
| $3^-$ | 2834.99(6) | 541.18(10) | k | 2294 | 2(1) | | $560^{+140}_{-100}$ | | |
| | | 609.1(2) | j | 2225 | 8(1) | $E1$ | | $2.5^{+9}_{-7} \times 10^{-4}$ | |
| | | 1509.49(4) | | 1326 | 79(2) | $E1$ | | $1.6^{+4}_{-4} \times 10^{-4}$ | |

TABLE II. *(Continued.)*

| $J^\pi$ | $E_x$ (keV) | $E_\gamma$ (keV) | Note | $E_f$ (keV) | BR (%) | $\delta$[a] | $\tau$ (fs) | $B(M1)/B(E1)$ (W.u.[b])/(W.u.)[c] | $B(E2)$ (W.u.)[d] |
|---|---|---|---|---|---|---|---|---|---|
| | | 2232.25(3) | | 603 | 11(1) | $E1$ | | $1^{+1}_{-1} \times 10^{-5}$ | |
| (5) | 2844.82(10) | 361.78(3) | g | 2483 | 30(5) | | $> 2$ ps | | |
| | | 1596.23(3) | | 1249 | 70(5) | | | | |
| | 2854.93(20) | 2252.2(20) | j | 603 | | | | | |
| | 2856.73(6) | 2254.0(5) | j | 603 | | | | | |
| $2^+$ | 2858.8(6) | 2255.98(5) | k | 603 | 97(1) | $-0.06^{+28}_{-28}$ | $110^{+10}_{-10}$ | $2.4^{+4}_{-3} \times 10^{-2}$ | $1.2^{+2}_{-2} \times 10^{-2}$ |
| | | 2858.50(25) | i | 0 | 3(1) | | | | $3.2^{+15}_{-13} \times 10^{-2}$ |
| (5,4) | 2862.9(12) | 1614.28(10) | i,l | 1249 | 100 | $+0.25^{+9}_{-10}$ | $170^{+20}_{-20}$ | $4.2^{+8}_{-6} \times 10^{-2}$ | $7.0^{+12}_{-10} \times 10^{-1}$ |
| (5) | 2865.31(12) | 531.31(4) | | 2335 | 100 | $+1.51^{+50}_{-34}$ | | | |
| | | | | | | $-1.54^{+38}_{-44}$ | | | |
| (6) | 2872.64(20) | 1624.06(20) | | 1249 | 100 | | $320^{+40}_{-30}$ | | $6.2^{+7}_{-7}$ |
| | 2873.20(11) | 1126.21(4) | j | 1747 | 100 | | $300^{+200}_{-100}$ | | |
| (6,5) | 2879.79(14) | 1132.80(10) | | 1747 | 100 | $-1.00^{+62}_{-28}$ | $130^{+140}_{-60}$ | | |
| | | | | | | $+0.95^{+27}_{-30}$ | | | |
| $3^-$ | 2885.93(8) | 846.4(20) | k | 2039(2) | 5(2) | $E1$ | $920^{+450}_{-240}$ | $4^{+3}_{-2} \times 10^{-5}$ | |
| | | 1559.80(3) | | 1326 | 15(2) | $E1$ | | $2^{+1}_{-1} \times 10^{-5}$ | |
| | | 1637.70(6) | | 1249 | 17(2) | $E1$ | | $2^{+1}_{-1} \times 10^{-5}$ | |
| | | 2283.25(10) | | 603 | 63(2) | $E1$ | | $2^{+1}_{-1} \times 10^{-5}$ | |
| $5^{(-)}$ | 2902.76(7) | 1654.18(4) | | 1249 | 100 | | | | |
| (5,4) | 2920.96(10) | 962.40(10) | i | 1958 | 57(2) | $+0.68^{+14}_{-20}$ | $> 470$ fs | $< 4 \times 10^{-2}$ | $<11$ |
| | | 1672.37(4) | | 1249 | 43(2) | $+0.30^{+14}_{-9}$ | | $< 6 \times 10^{-3}$ | $< 2 \times 10^{-1}$ |
| 6 | 2933.55(18) | 596.8(20) | j | 2335 | 81(5) | | | | |
| | | 1186.56(10) | | 1747 | 19(5) | | | | |
| | 2939.74(8) | 1691.15(6) | j,i | 1249 | | | | | |
| $2^+$ | 2946.5(16) | 906.29(10) | i,k | 2039(2) | 37(2) | $-0.92^{+56}_{-10}$ | $310^{+70}_{-60}$ | $2.8^{+20}_{-8} \times 10^{-2}$ | $20^{+7}_{-11}$ |
| | | 2343.01(16) | i | 603 | 36(3) | | | | |
| | | 2945.45(17) | i | 0 | 27(2) | | | | $8.8^{+30}_{-22} \times 10^{-2}$ |
| $(4^+)$ | 2958.6(14) | 1708.70(10) | i,l | 1249 | 82(2) | $+0.99^{+5}_{-6}$ | $270^{+70}_{-50}$ | $9.8^{+28}_{-24} \times 10^{-3}$ | $2.3^{+7}_{-6}$ |
| | | 2354.89(20) | i | 603 | 18(2) | | | | $2.1^{+8}_{-7} \times 10^{-1}$ |
| $(4^+)$ | 2963.5(10) | 923.29(6) | i,k | 2039(3) | 37(3) | $-0.09^{+12}_{-07}$ | | | |
| | | 1215.62(7) | i | 1747 | 35(4) | | | | |
| | | 2359.80(10) | i | 603 | 28(3) | | | | |
| | 2968.34(10) | 1221.35(8) | | 1747 | 100 | | | | |
| | 2973.7(15) | 1226.3(13) | j,k | 1747 | 100 | | | | |
| 1 | 2974.91(13) | 2371.91(20) | i,k | 603 | 14(3) | $E1$ | $51^{+6}_{-5}$ | $8^{+3}_{-2} \times 10^{-5}$ | |
| | | 2974.91(10) | | 0 | 86(3) | $E1$ | | $2.5^{+4}_{-3} \times 10^{-5}$ | |
| (3,4) | 2982.7(7) | 1657.22(5) | i,l | 1326 | 43(3) | $-0.13^{+13}_{-18}$ | $200^{+40}_{-30}$ | $1.5^{+4}_{-4} \times 10^{-2}$ | $6.4^{+17}_{-15} \times 10^{-2}$ |
| | | 1734.5(20) | i | 1249 | 13(3) | $+0.44^{+58}_{-35}$ | | $3.3^{+18}_{-16} \times 10^{-3}$ | $1.5^{+10}_{-7} \times 10^{-1}$ |
| | | 2379.02(4) | i | 603 | 44(2) | $+0.46^{+49}_{-22}$ | | $4.3^{+14}_{-17} \times 10^{-3}$ | $1.1^{+6}_{-4} \times 10^{-1}$ |

TABLE II. *(Continued.)*

| $J^\pi$ | $E_x$ (keV) | $E_\gamma$ (keV) | Note | $E_f$ (keV) | BR (%) | $\delta$[a] | $\tau$ (fs) | $B(M1)/B(E1)$ (W.u.[b])/(W.u.)[c] | $B(E2)$ (W.u.)[d] |
|---|---|---|---|---|---|---|---|---|---|
| 5 | 2986.66(8) | 1738.10(6) | | 1249 | 100 | $-0.19^{+16}_{-15}$ | $> 2$ ps | | |
| 1 | 2988.80(10) | 2386.10(9) | k | 603 | 75(2) | $+0.74^{+33}_{-68}$ | $130^{+20}_{-20}$ | $8.7^{+63}_{-28} \times 10^{-3}$ | $5.9^{+26}_{-32} \times 10^{-3}$ |
| | | 2988.80(5) | | 0 | 25(2) | | | $2.3^{+7}_{-5} \times 10^{-3}$ | |
| $3^-$ | 3001.12(11) | 707.02(6) | g,k | 2294 | 28(4) | $-0.22^{+13}_{-12}$ | $480^{+490}_{-180}$ | | |
| | | 1675.83(7) | | 1326 | 39(4) | $E1$ | | $7^{+5}_{-4} \times 10^{-5}$ | |
| | | 1752.20(3) | | 1249 | 33(4) | $E1$ | | $5^{+4}_{-3} \times 10^{-5}$ | |
| | 3028.16(25) | 1702.27 | g,i,l | 1326 | 65(5) | | | | |
| | | 2425.34(33) | i | 603 | 35(5) | | | | |
| | 3045.55(22) | 2442.82(22) | | 603 | 100 | | $960^{+860}_{-330}$ | | |
| | 3049.63(12) | 2446.90(12) | i,k,l | 603 | 100 | | | | |
| 3 | 3054.75(16) | 1729.23(14) | i,k,l | 1326 | 45(6) | $-0.36^{+24}_{-51}$ | $200^{+50}_{-40}$ | | |
| | | 1806.46(15) | i | 1249 | 55(6) | | | | |
| | 3075.67(20) | 1117.95(3) | i,k,l | 1958 | 10(1) | | | | |
| | | 1826.81(20) | i | 1249 | 90(1) | | | | |
| (4,5,6) | 3077.14(8) | 1330.00(6) | i,l | 1747 | | | | | |
| | 3084.3(10) | 1834.38(8) | g,i,k,l | 1249 | 74(1) | | $250^{+70}_{-50}$ | | |
| | | 2480.55(7) | i | 603 | 26(1) | | | | |
| 1 | 3090.7(14) | 2486.42(10) | k | 603 | 33(1) | | $< 4$ fs | | |
| | | 3090.69(15) | | 0 | 67(1) | | | | |
| | 3095.41(16) | 1769.42(15) | k | 1326 | 41(1) | | $620^{+2970}_{-310}$ | | |
| | | 2492.59(40) | | 603 | 59(1) | | | | |
| $(2^-)$ | 3101.40(13) | 354.35(12) | k | 2747 | | | | | |
| | 3107.21(14) | 1781.99(12) | i,l | 1326 | $> 25$ | | $120^{+30}_{-30}$ | | |
| | | 1858.1(6) | j,i | 1249 | $< 48$ | | | | |
| | | 2504.49(25) | i | 603 | $> 26$ | | | | |
| | | 3106.70(41) | i,m | 0 | $< 1$ | | | | |
| | 3109.43(9) | 1860.85(6) | i,l | 1249 | | | $240^{+50}_{-40}$ | | |
| | [3117.46(36)] | [3117.46(36)] | m | 0 | | | | | |
| (3) | 3118.08(12) | 1792.08(23) | i | 1326 | 21(1) | | $130^{+20}_{-20}$ | | |
| | | 1868.52(20) | i | 1249 | 18(1) | $+0.68^{+24}_{-32}$ | | | |
| | | 2515.78(3) | i | 603 | 61(1) | | | | |
| (3) | 3142.82(8) | 1894.33(9) | i,k,l | 1249 | 30(2) | | $220^{+50}_{-40}$ | | |
| | | 2539.97 | i | 603 | 70(2) | $-0.51^{+48}_{-39}$ | | | |
| (2) | 3159.26(10) | 1834.25(8) | i,k | 1326 | 71(2) | | $270^{+50}_{-40}$ | | |
| | | 2556.01(23) | i | 603 | 12(2) | | | | |
| | | 3159.17(11) | i | 0 | 17(2) | | | | |
| (3) | 3163.48(18) | 2560.75(17) | i,k | 603 | | $-0.24^{+25}_{-132}$ | | | |
| (3) | 3167.25(12) | 1841.77(10) | k | 1326 | | $-0.58^{+53}_{-32}$ | $> 2$ ps | | |
| (4) | 3177.73(7) | 2574.34(22) | i,k | 603 | | | | | |

TABLE II. *(Continued.)*

| $J^\pi$ | $E_x$ (keV) | $E_\gamma$ (keV) | Note | $E_f$ (keV) | BR (%) | $\delta$[a] | $\tau$ (fs) | $B(M1)/B(E1)$ (W.u.[b]/(W.u.)[c] | $B(E2)$ (W.u.)[d] |
|---|---|---|---|---|---|---|---|---|---|
| 3(2) | 3212.13(7) | 2609.31(6) | k | 603 | | | $120^{+30}_{-30}$ | | |
| | 3218.41(7) | 2615.59(6) | k | 603 | | | | | |
| 1 | 3221.16(7) | 2617.41(5) | k | 603 | 53(10) | | $60^{+20}_{-30}$ | | |
| | | 3221.16(7) | | 0 | 47(10) | | | | |
| | 3238.0(12) | 2635.16(12) | k | 602 | 71(4) | | | | |
| | | 3238.0(11) | | 0 | 29(4) | | | | |
| | 3257.8(32) | 3257.8(32) | i,k | 0 | | | | | |
| | 3290.32(20) | 3290.32(20) | i,k | 0 | | | | | |

[a]In situations where $\chi^2$ vs $\tan^{-1}\delta$ plots yield two equivalent solutions for the multipole-mixing ratio, the $\delta$ from the first value has been used to calculate electromagnetic transition rates and is listed first in the table.
[b]$B(M1)_{W.u.}$=1.7905 $\mu_N^2$.
[c]$B(E1)_{W.u.}$=1.6021 e$^2$ fm$^2$.
[d]$B(E2)_{W.u.}$=36.691 e$^2$ fm$^4$.
[e]From Ref. [8].
[f]From Ref. [12].
[g]Branching ratios are from excitation functions.
[h]See level discussion.
[i]New transition.
[j]Assignment from coincidence data.
[k]Calculations show strength is probably missing from this level.
[l]New level.
[m]Seen only in the summed angle data.

3 MeV labeled as new may correspond to previously observed levels with large energy uncertainties [11].

### A. 2092.0-keV $2_4^+$ level

A $\gamma$ ray to the ground state is clearly observed for this level, in agreement with Ref. [5]. The 843.7-keV $\gamma$ ray reported in Ref. [9] is below the detection threshold of these measurements.

### B. 2182.5-keV $1^{(+)}$ level

The angular distribution and the excitation function of the 2182.5-keV $\gamma$ ray emitted in the ground-state decay of this level indicate $J = 1$, as shown in Figs. 2 and 3; this assignment differs from the adopted value of $J = 2$ [11] but agrees with Ref. [9]. The tentative positive-parity assignment is from Ref. [9]. The systematic behavior of the excitation energies and $B(M1;\ 1^+ \rightarrow 0_1^+)$ values of this lowest $1^{(+)}$ excitation observed in $^{122-130}$Te was reported earlier and can be viewed in Fig. 7 of Ref. [30].

### C. 2483.3-keV $4^{(-)}$ level

The 1234.2-keV $\gamma$ ray assigned to this level in Ref. [9] is weakly observed in the 646-keV coincidence gate in this work, but it is not resolved in the angular distribution and excitation function data.

The adopted spin parity of this level is $3^+$ [11], which is also the $J^\pi$ listed in Ref. [9]. Warr *et al.* [6] proposed $J^\pi = 4^{(-)}$, provided the 2039-keV level is a doublet and provided this state decays to the $3^+$ member of that doublet, which is now known to be the case.

The observed 444.0-keV $\gamma$ ray is complicated by a 443.6-keV contaminant line from $^{125}$Te. The 443.6-keV level in $^{125}$Te decays by either 443.6- or 408.1-keV transitions, both of which are seen in the current data. Using the known $\gamma$-ray branching ratios [11] for this $^{125}$Te level, the 443.6-keV contaminant peak was subtracted to obtain the yield of the 444.0-keV $\gamma$ ray in $^{124}$Te as a function of incident neutron energy. Using branching ratios from Ref. [9], statistical model calculations, and the excitation functions from the 525.4- and corrected 444.0-keV levels, the spin of this level is $J = 4$. The $(-)$ parity assignment is taken from Ref. [6].

### D. 2529.9-keV $0^+$ level

This level has an adopted spin $J^\pi = 2^+$ [11], in agreement with Ref. [9]. The angular distribution and excitation function of the 1927.1-keV $\gamma$ ray observed in this work indicate the level has a spin $J = 0$, which is in agreement with Ref. [31]. This level was not observed by Warr *et al.* [6] in $(\alpha,2n\gamma)$ measurements, which further supports the J = 0 spin assignment, as does the excitation function of the 1927.1-keV $\gamma$ ray compared to statistical model calculations shown in Fig. 3. Positive parity is deduced from the $E2$ decay into the $2_1^+$ level.

### E. 2665.5-keV $6^+$ level

Levels are adopted [11] at 2664.3 ($J^\pi = 6^+$) and 2665.1 keV ($J^\pi = 8^+$) with transitions of 329.3 and 918.1 keV, respectively. These new data support two transitions from a level at 2665.5 keV with energies of 329.8 and 918.1 keV. The angular distributions of both $\gamma$ rays support $J = 6$, as do the excitation functions when compared to CINDY calculations. Since $J = 8$ levels are rarely populated in $(n,n'\gamma)$ measurements, this does not exclude the $J = 8$ state at 2665.1 keV, but rather a new transition is assigned to the lower spin state.

### F. 2681.5-keV $2^+$ level

This level has adopted $\gamma$ rays of 2078.8 and 346.5 keV, with the latter having a strength of about 20% of the former. We see a 2078.5-keV $\gamma$ ray and a new ground-state branch, but in agreement with Ref. [6], we see no evidence of the 346.5-keV $\gamma$ ray.

### G. 2709.5-keV level

A 2709.5-keV $\gamma$ ray is seen only in the summed angle data. Based only on energetics, this transition is assumed to be a ground-state transition.

### H. 2710.8-keV 3 level

The angular distributions of both the 1385.2- and 2108.1-keV $\gamma$ rays support a $J = 3$ spin assignment for this level, in agreement with Ref. [11]. No indication of a 962.4-keV $\gamma$ ray from this level was observed in this work, as found in Ref. [6], or the 662.1-keV $\gamma$ ray listed in Ref. [9]; the 962.4-keV $\gamma$ ray observed in this work is assigned to the 2921.0-keV level based on its excitation function and its presence in the 709-keV coincidence gate. Statistical model calculations indicate, however, that strength is still missing if this is a $J = 3$ state.

### I. 2713.3-keV (5) level

Warr *et al.* [6] assign a 966-keV $\gamma$ ray to a level at 2713.7 keV with $J = (5–7)$. A 1464.9-keV $\gamma$ ray is observed in this work with a tentative spin of $J = 5$. We do not see a 966-keV $\gamma$ ray in the appropriate coincidence gate.

### J. 2734.0-keV (5,4) level

The level was proposed in Ref. [32] based on its decay via a 774.83-keV $\gamma$ ray, which was later refuted [33]. A level at this energy is definitely confirmed in the present work by a 1485.4-keV $\gamma$ ray in the 646-keV coincidence gate, as shown in Fig. 1 and in Ref. [9]. A 775.3-keV $\gamma$ ray observed in this work, however, clearly belongs to the 2814.7-keV level.

### K. 2774.3-keV $6^+$ and 2775.0-keV $3^-$ levels

A doublet is observed at this energy in agreement with Ref. [6]. $\gamma$ rays of 1026.9 and 1526.2 keV have angular distributions that indicate $J = 6$ for the originating level. Additional $\gamma$ rays of 480.6, 735.3, and 816.8 keV are observed from a level at 2774 keV. The first two have angular distributions that prefer $J = (3,4)$ and are assigned to a $J^\pi = 3^-$ level in agreement with Refs. [6,11]. The angular distribution observed in this work for the 816.8-keV $\gamma$ ray does not exclude its placement with either level, but we place it with the $3^-$ level in agreement with Refs. [6,11]. The 1526.2-keV $\gamma$ ray is assigned to both levels as its strength substantially exceeds that calculated for a $J = 6$ state. The $\gamma$-ray branchings given for these two levels are determined by using the statistical model calculations to distribute the strength of the 1526.2-keV $\gamma$ ray assuming only two transitions occur from the $J = 6$ level. Calculations indicate that strength from the $J = 3$ level is still missing.

### L. 2865.3-keV (5) level

The angular distribution and excitation function of the 531.3-keV $\gamma$ ray observed in this work indicate $J = 5$ as the preferred spin, which differs from the adopted spin $J = 3$ [11].

### M. 2897.3-keV 1,($2^+$) level

A level was adopted [11] at this energy with a ground-state decay. No $\gamma$ ray is observed of the appropriate energy, in this work in agreement with Refs. [6,9].

Comparisons between statistical model calculations for $\gamma$-ray production cross sections and the experimental data become difficult above 2.9 MeV, either because of model limitations or a lack of complete knowledge of the levels and their decays.

## IV. DISCUSSION

Critical-point symmetry occurs in a quantal system when a phase transition takes place between dynamical symmetries, e.g., vibrational [$U(5)$] to $\gamma$-soft rotational [$O(6)$] in nuclear systems [15,20]. This occurs in a geometric model when the potential energy $U(\beta,\gamma)$ is separable in $\beta$ and $\gamma$, and it is evinced in a nucleus when the agreement between experimental observables and geometric-model calculations is independent of the variable $\gamma$. The generalized collective model (GCM) was used to establish the $\gamma$ independence of geometric-model calculations for $^{124}$Te, and also for $^{122}$Te [21] and $^{126}$Te [22]. The results of these new calculations are discussed below. Other characteristics of a nucleus undergoing a critical-point phase transition are identified in Ref. [18]. $0^+$ levels and their decay characteristics are key identifiers of nuclear symmetries, and states are identified in the $E(5)$ or $\beta^4$ critical-point symmetries by two quantum numbers: $\xi$ labels major families and $\tau$ labels phonon-like structure within each major family. Then new experimental results for $^{124}$Te are compared to $E(5)$ and $\beta^4$-potential critical-point symmetry observables. Similar comparisons are made for $^{122}$Te and $^{126}$Te.

### A. Generalized collective model (GCM)

The GCM [34–38] can be used to describe the collective motion of nuclei. The Gneuss-Greiner form [34] of the GCM potential energy may be expressed in terms of the standard

TABLE III. Energy ratios for the $E(5)$ [18] and $\beta^4$ critical point symmetries from Ref. [20] along with experimental values for $^{122,124,126}$Te [21,22].

| Exp $(0_2^+, 0_3^+)$ | $E(5)$ | $\beta^4$ | 122 | 124 | 126 |
|---|---|---|---|---|---|
| $E(4_1^+)/E(2_1^+)$ | 2.20 | 2.09 | 2.09 | 2.07 | 2.04 |
| $E(0_\xi^+)/E(2_1^+)$ | 3.03 | 2.39 | 2.41 | 2.75 | 2.81 |
| $E(0_\tau^+)/E(2_1^+)$ | 3.59 | 3.27 | 3.10 | 3.12 | 3.17 |
| $E(0_\xi^+)/E(0_\tau^+)$ | 0.84 | 0.73 | 0.78 | 0.88 | 0.89 |

polar intrinsic deformation variables $\beta$ and $\gamma$ by

$$V(\beta,\gamma) = C_2\sqrt{\frac{1}{5}}\beta^2 - C_3\sqrt{\frac{2}{35}}\beta^3\cos(3\gamma) + C_4\frac{1}{5}\beta^4. \quad (2)$$

Different macroscopic collective motions can be investigated with one potential energy in this model, with the underlying symmetry determined from the values of the fitting parameters $C_2$, $C_3$, and $C_4$.

This model was used to investigate collective excitations in $^{122}$Te, $^{124}$Te, and $^{126}$Te. For these nuclei, a reasonable set of parameters was found to be (in MeV) $C_2 = 0 \pm 250$, $C_3 = 0 \pm 1000$, and $C_4 = 34000 \pm 2000$. The overall goodness of fit to low-lying excited levels is in general insensitive to $C_2$ and $C_3$ within the range listed, since variations in these parameters improve some characteristics of the calculated level scheme while worsening others. Since $C_4$ is the only parameter that significantly affects the level scheme, the potential energy is essentially proportional to $\beta^4$; this observation is consistent with previous investigations of nuclei in this mass region [39,40] and with dynamic deformation model calculations that support both $^{122}$Te and $^{124}$Te as $\gamma$-soft nuclei [41]. Such $\gamma$ independence in model calculations when describing experimental level energies makes $^{122}$Te, $^{124}$Te, and $^{126}$Te good candidates in which to investigate critical-point phenomena between the $U(5)$ and $O(6)$ symmetries [13,15,18,20].

### B. Critical-point symmetries

The strong dependence on the $\beta^4$ term found in the GCM Hamiltonian for $^{122,124,126}$Te calculations supports comparing observed spectral properties with predictions of the $E(5)$ symmetry and $\beta^4$ potential at the critical point. The closed-form solutions for both the $E(5)$ dynamic symmetry [18] and the $\beta^4$ potential [20] provide an easy method for evaluating the models, provided the low-lying level spins, parities, and reduced transition probabilities are known. Some of the key $E(5)$ and $\beta^4$ model energy ratios are listed in Table III, along with experimental values for $^{122}$Te, $^{124}$Te, and $^{126}$Te. The identification of the lowest $0^+$ states and the $B(E2)$ values of their decays are considered most important in evaluating critical-point phenomena [42–45].

The closed-form $B(E2)$s from $E(5)$ and $\beta^4$ potential-model calculations are given in Table IV and shown in Fig. 5 in comparison to experimental values for $^{124}$Te. While some energy ratios and $B(E2)$ values agree well with the critical-point symmetry model predictions, the critical decays of the $0^+$ levels are not in agreement with model calculations. In general, however, the $E(5)$ model predictions for $B(E2)$ values agree more closely with experiment than $\beta^4$ potential-model calculations.

TABLE IV. Comparisons of experimental $B(E2)$ values with $E(5)$ [18] and $\beta^4$ potential critical-point symmetry model calculations. All transition rates are in W.u.

| $B(E2; J_i^+ \to J_f^+)$ | Exp. | $(\tau,\xi)_i \to (\tau,\xi)_f$ | $E(5)$ | $\beta^4$ |
|---|---|---|---|---|
| $B(E2; 2_1^+ \to 0_1^+)$ | 31.1(5)[a] | (1,1)→(0,1) | 31.1 | 31.1 |
| $B(E2; 4_1^+ \to 2_1^+)$ | $35.9^{+17}_{-17}$[b] | (2,1)→(1,1) | 49.0 | 56.6 |
| $B(E2; 2_2^+ \to 0_1^+)$ | $0.83^{+23}_{-16}$ | (2,1)→(0,1) | 0.9 | 0 |
| $B(E2; 2_2^+ \to 2_1^+)$ | $22.1^{+45}_{-43}$ | (2,1)→(1,1) | 49.0 | 56.6 |
| $B(E2; 0_2^+ \to 2_1^+)$ | 14.3(29) | (0,2)→(1,1) | 15.2 | 43.9 |
| $B(E2; 6_1^+ \to 4_1^+)$ | | (2,1)→(1,1) | 60.3 | 78.4 |
| $B(E2; 0_3^+ \to 2_1^+)$ | | (3,1)→(1,1) | 1.9 | 78.4 |
| $B(E2; 0_3^+ \to 2_2^+)$ | $350^{+70}_{-100}$[a] | (3,1)→(2,1) | 60.3 | 0 |
| $B(E2; 3_1^+ \to 2_1^+)$ | | (3,1)→(1,1) | 0 | 0 |
| $B(E2; 3_1^+ \to 2_2^+)$ | $59^{+10}_{-10}$[a] | (3,1)→(2,1) | 43.0 | 56.0 |
| $B(E2; 3_1^+ \to 4_1^+)$ | | (3,1)→(2,1) | 0 | 56.0 |
| $B(E2; 4_2^+ \to 2_1^+)$ | $4.3^{+9}_{-9}$ | (3,1)→(1,1) | 0 | 0 |
| $B(E2; 4_2^+ \to 2_2^+)$ | $14.1^{+30}_{-28}$ | (3,1)→(2,1) | 31.7 | 41.1 |
| $B(E2; 4_2^+ \to 4_1^+)$ | $12.7^{+74}_{-58}$ | (3,1)→(2,1) | 18.2 | 37.3 |

[a]Adopted values from Ref. [11].
[b]Adopted values from Ref. [12].

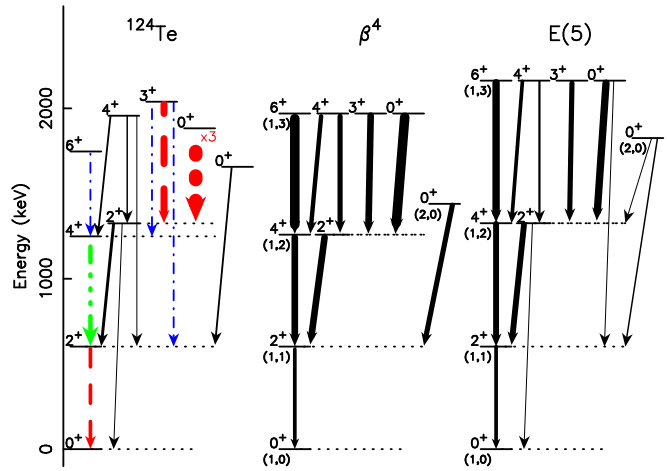


FIG. 5. Experimental low-lying positive-parity levels and $B(E2)$ values in $^{124}$Te compared to predicted values from $\beta^4$ potential [20] and $E(5)$ critical-point symmetry calculations [15,18]. The dashed lines (red) are observed transitions for which $B(E2)$ values are from Ref. [11]; the dot-dashed lines (blue) are observed transitions for which $B(E2)$ values have not been determined; the dot-dot-dot-dashed lines (green) represent $B(E2)$ values from Ref. [12]; and the solid and dashed (upper limits) black lines are from this work. The ordered pairs under the levels correspond to $(\xi,\tau)$ in $\beta^4$ and $E(5)$ symmetry calculations.

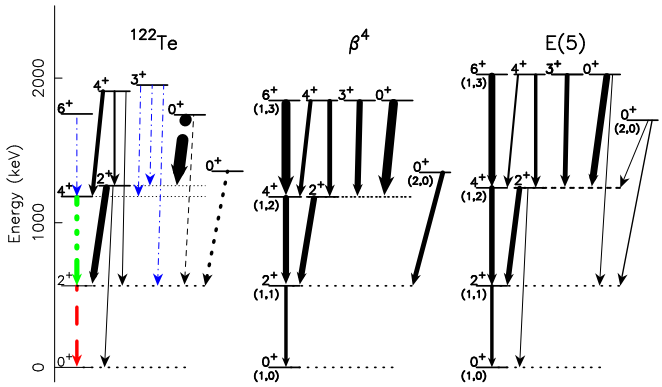


FIG. 6. Experimental low-lying positive-parity levels and $B(E2)$ values in $^{122}$Te compared to predicted values from $\beta^4$ potential [20] and $E(5)$ critical-point symmetry calculations [15,18]. The dot-dashed lines (blue) are observed transitions for which $B(E2)$ values have not been determined; the dashed lines (red) are observed transitions for which $B(E2)$ values are from Ref. [46]; the dot-dot-dot-dashed lines (green) represent $B(E2)$ values from Ref. [12]; and the solid and dashed (upper limits) black lines represent values from Ref. [21]. The ordered pairs under the levels correspond to $(\xi,\tau)$ in $\beta^4$ and $E(5)$ symmetry calculations.

Comparisons of experimental energy levels and $B(E2)$ values with critical-point symmetry-model calculations for neighboring $^{122}$Te and $^{126}$Te, respectively, are shown in Figs. 6 and 7. For Figs. 5, 6, and 7 model predictions for energies and transitions are from Refs. [18,20] and are relative to that observed for the $2_1^+$ level energy and the $B(E2; 2_1^+ \rightarrow 0_1^+)$ value, which are $E(2_1^+) = 564$, 602, and 666 keV and $B(E2; 2_1^+ \rightarrow 0_1^+) = 37.0$, 31.1, and 25.4 W.u. for $^{122}$Te, $^{124}$Te, and $^{126}$Te, respectively. The level energies and the widths of the arrows are normalized to the $2_1^+$ energy and $B(E2; 2_1^+ \rightarrow 0_1^+)$ value for each nucleus, respectively, thus all $B(E2; 2_1^+ \rightarrow 0_1^+)$ transitions have the same arrow widths and comparisons are valid only within an individual figure.

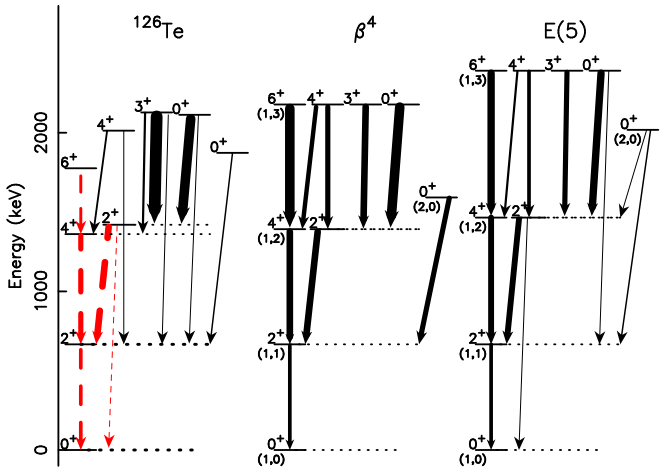


FIG. 7. Experimental low-lying positive-parity levels and $B(E2)$ values in $^{126}$Te compared to predicted values from $\beta^4$ potential [20] and $E(5)$ critical-point symmetry calculations [15,18]. The dashed lines (red) are observed transitions for which $B(E2)$ values are from Ref. [47] and the black lines represent values from Ref. [22]. The ordered pairs under the levels correspond to $(\xi,\tau)$ in $\beta^4$ and $E(5)$ symmetry calculations.

The energy comparisons in Table III and Figs. 5, 6, and 7 indicate that many of the decay characteristics of these nuclei are well described by the $E(5)$ symmetry, especially the magnitude of the $B(E2; 0_2^+ \rightarrow 2_1^+)$ value, although the decay of this level into the $2_2^+$ state predicted by the $E(5)$ picture is not observed for any of these nuclei; this transition is not predicted to occur in the $\beta^4$-potential model. The large $B(E2; 0_3^+ \rightarrow 2_2^+)$ value observed in $^{124}$Te [8] is not well described by either the $E(5)$ or $\beta^4$-potential critical-point calculations, while in $^{122,126}$Te both transitions from the $0_3^+$ level predicted by the $E(5)$ calculations are observed and the experimental and model $B(E2)$ values are in good agreement. The $B(E2; 4_1^+ \rightarrow 2_1^+)$ values for $^{124}$Te and $^{126}$Te are underpredicted by the models by about a third, but for $^{122}$Te the $E(5)$ model predictions agree very well with the observed value. The large number of observed $\tau = 3$ to $\tau = 2$ transitions are not predicted by either the $E(5)$ or $\beta^4$-potential critical-point symmetry calculations. Overall, each of these nuclei is reasonably well described by the $E(5)$ model, but the prediction of Ref. [18] that $^{124}$Te is the best $E(5)$ candidate is not supported by the model comparisons, as the very important decays of the $0^+$ levels agree with the $E(5)$ model predictions more closely in both $^{122}$Te and $^{126}$Te. The $\beta^4$-potential critical-point calculations are not as successful in describing the experimental observations in any of these nuclei, as several more decays are seen experimentally than are predicted by the model.

## V. SUMMARY

Levels of $^{124}$Te up to 3.3 MeV in excitation have been examined using the variety of tools available with the $(n,n'\gamma)$ reaction. Over 95 levels were observed and lifetimes were found for 51 levels; limits were placed on 10 others; $\gamma$-ray branching ratios, multipole-mixing ratios, level spins, and transition probabilities were also determined for these levels. The new $B(E2)$ values deduced from these experimental data provided information necessary for evaluating critical-point phase transitions in $^{122,124,126}$Te. Many decay characteristics of the lowest excited levels of $^{124}$Te, as well as those of $^{122}$Te and $^{126}$Te, are well described by the $E(5)$ critical-point symmetry model calculations. The important decays of low-lying $0^+$ levels in $^{122}$Te and $^{126}$Te are better described by the $E(5)$ critical-point symmetry model than is observed in $^{124}$Te.

## ACKNOWLEDGMENTS

Support of this project by the Department of Energy through NNSA/SSAA Grant No. DE-NA0002931 and the National Science Foundation through Grants No. PHY-9600431, No. PHY-9626846, and No. PHY-1606890 is gratefully acknowledged. We also acknowledge with appreciation discussions with M. T. McEllistrem and the maintenance of the UKAL by H. E. Baber.

[1] J. Rikovska, N. J. Stone, P. M. Walker, and W. B. Walters, Nucl. Phys. A **505**, 145 (1989).
[2] R. F. Casten, J.-Y. Zhang, and B.-C. Liao, Phys. Rev. C **44**, 523 (1991).
[3] C. S. Lee, J. A. Cizewski, D. Barker, R. Tanczyn, G. Kumbartzki, J. Szczepanski, J. W. Gan, H. Dorsett, R. G. Henry, L. P. Farris, and H. Li, Nucl. Phys. A **528**, 381 (1991).
[4] J. A. Cizewski, L. A. Bernstein, R. G. Henry, H. Q. Jin, C. S. Lee, and W. Younes, in *Proceedings of the 8th International Symposium on Capture Gamma-Ray Spectroscopy and Related Topics*, edited by J. Kern (World Scientific, Singapore, 1994), p. 328.
[5] R. Georgii, T. von Egidy, J. Klora, H. Lindner, U. Mayerhofer, J. Ott, W. Schauer, P. von Neumann-Cosel, A. Richter, C. Schlegel, R. Schulz, V. A. Khitrov, A. M. Sukhovoj, A. V. Vojnov, J. Berzins, V. Bondarendo, P. Prokofjevs, L. J. Simonova, M. Grinberg, and C. Stoyanov, Nucl. Phys. A **592**, 307 (1995).
[6] N. Warr, S. Drissi, P. E. Garrett, J. Jolie, J. Kern, H. Lehmann, S. J. Mannanal, and J.-P. Vorlet, Nucl. Phys. A **636**, 379 (1998).
[7] W. Schauer, C. Doll, T. von Egidy, R. Georgii, J. Ott, H.-F. Wirth, A. Gollwitzer, G. Graw, R. Hertenberger, B. Valnion, M. Grinberg, and C. Stoyanov, Nucl. Phys. A **652**, 339 (1999).
[8] C. Doll, H. Lehmann, H. G. Börner, and T. von Egidy, Nucl. Phys. A **672**, 3 (2000).
[9] T. von Egidy, H.-F. Wirth, I. Tomandl, and J. Honzátko, Phys. Rev. C **74**, 034319 (2006).
[10] A. Patil, D. Santhosh, K. V. Sai, M. Sainath, and K. Venkataramaniah, Appl. Radiation Isotopes **64**, 693 (2006).
[11] H. Iimura, J. Katakura, K. Kitao, and T. Tamura, Nucl. Data Sheets **80**, 895 (1997).
[12] M. Saxena, R. Kumar, A. Jhingan, S. Mandal, A. Stolarz, A. Banerjee, R. K. Bhowmik, S. Dutt, J. Kaur, V. Kumar, M. Modou Mbaye, V. R. Sharma, and H.-J. Wollersheim, Phys. Rev. C **90**, 024316 (2014).
[13] H. Sabri, Z. Jahangiri, and M. A. Mohammadi, Nucl. Phys. A **946**, 11 (2016).
[14] A. Kerek, Nucl. Phys. A **176**, 466 (1971).
[15] F. Iachello, Phys. Rev. Lett. **85**, 3580 (2000).
[16] F. Iachello, Phys. Rev. Lett. **87**, 052502 (2001).
[17] A. Bohr and B. R. Mottelson, *Nuclear Structure* (Benjamin, W. A. Inc., Reading, MA, 1975), Vol. II.
[18] R. M. Clark, M. Cromaz, M. A. Deleplanque, M. Descovich, R. M. Diamond, P. Fallon, I. Y. Lee, A. O. Macchiavelli, H. Mahmud, E. Rodriguez-Vieitez, F. S. Stephens, and D. Ward, Phys. Rev. C **69**, 064322 (2004).
[19] R. F. Casten and N. V. Zamfir, Phys. Rev. Lett. **85**, 3584 (2000).
[20] J. M. Arias, C. E. Alonso, A. Vitturi, J. E. García-Ramos, J. Dukelsky, and A. Frank, Phys. Rev. C **68**, 041302 (2003).
[21] S. F. Hicks, G. K. Alexander, C. A. Aubin, M. C. Burns, C. J. Collard, M. M. Walbran, J. R. Vanhoy, E. Jensen, P. E. Garrett, M. Kadi, A. Martin, N. Warr, and S. W. Yates, Phys. Rev. C **71**, 034307 (2005).
[22] J. R. Vanhoy, J. A. Tanyi, K. A. Crandell, T. H. Churchill, S. F. Hicks, M. C. Burns, P. A. Roddy, N. V. Warr, T. B. Brown, and S. R. Lesher, Phys. Rev. C **69**, 064323 (2004).
[23] C. A. McGrath, P. E. Garrett, M. F. Villani, and S. W. Yates, Nucl. Instrum. Methods Phys. Res., Sect. A **421**, 458 (1999).
[24] P. E. Garrett, N. Warr, and S. W. Yates, J. Res. Natl. Inst. Stand. Technol. **105**, 141 (2000).
[25] E. Sheldon and D. M. Van Patter, Rev. Mod. Phys. **38**, 143 (1966).
[26] R. W. Harper, T. W. Godfrey, and J. L. Weil, Phys. Rev. C **26**, 1432 (1982).
[27] K. B. Winterbon, Nucl. Phys. A **246**, 293 (1975).
[28] T. Belgya, G. Molnár, and S. W. Yates, Nucl. Phys. A **607**, 43 (1996).
[29] S. F. Hicks, J. R. Vanhoy, and S. W. Yates, Phys. Rev. C **78**, 054320 (2008).
[30] S. F. Hicks, J. C. Boehringer, N. Boukharouba, C. Fransen, S. R. Lesher, J. M. Mueller, J. R. Vanhoy, and S. W. Yates, Phys. Rev. C **86**, 054308 (2012).
[31] T. Tamura, K. Miyano, and S. Ohya, Nucl. Data Sheets **41**, 413 (1984).
[32] G. Mardirosian and N. M. Stewart, Z. Phys. A **315**, 213 (1984).
[33] Y. Jianming, L. Yunzuo, and H. Dailing, Z. Phys. A **331**, 391 (1988).
[34] G. Gneuss and W. Greiner, Nucl. Phys. A **171**, 449 (1971).
[35] J. M. Eisenberg and W. M. Greiner, *Nuclear Theory, Volume 1: Nuclear Models*, 3rd ed. (North-Holland, Amsterdam, 1987).
[36] P. O. Hess, M. Seiwert, J. A. Maruhn, and W. Greiner, Z. Phys. A **296**, 147 (1980).
[37] D. Troltenier, J. A. Maruhn, and P. O. Hess, *Computational Nuclear Physics 1: Nuclear Structure* (Springer-Verlag, New York, 1991).
[38] D. Troltenier, J. A. Maruhn, W. Greiner, V. Velazquez Aguilar, P. O. Hess, and J. H. Hamilton, Z. Phys. A **338**, 261 (1991).
[39] M. A. Caprio, R. F. Casten, and J. Jolie, Phys. Rev. C **65**, 034304 (2002).
[40] Y. Alhassid, G. F. Bertsch, D. J. Dean, and S. E. Koonin, Phys. Rev. Lett. **77**, 1444 (1996).
[41] A. R. H. Subber, P. Park, W. D. Hamilton, K. Kumar, K. Schreckenbach, and G. Colvin, J. Phys. G **12**, 881 (1986).
[42] L. Coquard, N. Pietralla, T. Ahn, G. Rainovski, L. Bettermann, M. P. Carpenter, R. V. F. Janssens, J. Leske, C. J. Lister, O. Möller, W. Rother, V. Werner, and S. Zhu, Phys. Rev. C **80**, 061304 (2009).
[43] L. Coquard, N. Pietralla, G. Rainovski, T. Ahn, L. Bettermann, M. P. Carpenter, R. V. F. Janssens, J. Leske, C. J. Lister, O. Möller, W. Rother, V. Werner, and S. Zhu, Phys. Rev. C **82**, 024317 (2010).
[44] D. Bonatsos, D. Lenis, N. Pietralla, and P. A. Terziev, Phys. Rev. C **74**, 044306 (2006).
[45] E. E. Peters, T. J. Ross, S. F. Ashley, A. Chakraborty, B. P. Crider, M. D. Hennek, S. H. Liu, M. T. McEllistrem, S. Mukhopadhyay, F. M. Prados-Estévez, A. P. D. Ramirez, J. S. Thrasher, and S. W. Yates, Phys. Rev. C **94**, 024313 (2016).
[46] T. Tamura, Nucl. Data Sheets **71**, 461 (1994).
[47] J. Katakura and K. Kitao, Nucl. Data Sheets **97**, 765 (2002).